12-1-2010

Aortic Coarctation: Recent Developments in Experimental and Computational Methods to Assess Treatments for this Simple Condition

John F. LaDisa
Marquette University, john.ladisa@marquette.edu

Charles A. Taylor
Departments of Bioengineering and Pediatrics

Jeffrey A. Feinstein
Departments of Bioengineering and Pediatrics

Accepted version. *Progress in Pediatric Cardiology*, Volume 30, No. 1-2 (December 2010), DOI.

Aortic Coarctation: Recent Developments in Experimental and Computational Methods to Assess Treatments for This *Simple* Condition

John F. LaDisa, Jr.
Department of Biomedical Engineering, Marquette University
Department of Pediatrics, Children's Hospital of Wisconsin
Milwaukee, WI
Charles A. Taylor
Department of Bioengineering, Stanford University and Lucile Packard Children's Hospital
Stanford, CA
Jeffrey A. Feinstein
Department of Bioengineering, Stanford University and Lucile Packard Children's Hospital
Department of Pediatrics, Stanford University and Lucile Packard Children's Hospital
Stanford, CA

Abstract

Coarctation of the aorta (CoA) is often considered a relatively simple disease, but long-term outcomes suggest otherwise as life expectancies are decades less than in the average population and substantial morbidity often exists. What follows is an expanded version of collective work conducted by the authors' and numerous collaborators that was presented at the 1st

Progress in Pediatric Cardiology, Vol. 30, No. 1-2 (December 2010): pg. 45-49. DOI.

International Conference on Computational Simulation in Congenital Heart Disease pertaining to recent advances for CoA. The work begins by focusing on what is known about blood flow, pressure and indices of wall shear stress (WSS) in patients with normal vascular anatomy from both clinical imaging and the use of computational fluid dynamics (CFD) techniques. Hemodynamic alterations observed in CFD studies from untreated CoA patients and those undergoing surgical or interventional treatment are subsequently discussed. The impact of surgical approach, stent design and valve morphology are also presented for these patient populations. Finally, recent work from a representative experimental animal model of CoA that may offer insight into proposed mechanisms of long-term morbidity in CoA is presented.

Coarctation of the aorta (CoA) accounts for 8 to 11% of congenital heart defects resulting in between 3,000 and 5,000 patients annually in the United States (1, 7). Current methods of treatment including surgery and stenting can alleviate the blood pressure (BP) gradient across a coarctation and are associated with low morbidity (3, 11, 21), but long-term results are inconsistent with the putative notion of CoA as a simple disease since life expectancies are decades less than in the average population (3, 24) and substantial morbidity exists in the form of hypertension, early onset coronary artery disease, stroke and aneurysm formation (5, 10, 13).

In 1971, O'Rourke and Cartmill suggested CoA-induced morbidity could be explained on the basis of abnormal hemodynamics and vascular biomechanics (19). Recent clinical literature has lost sight of this hemodynamic basis for the morbidity in CoA patients. At the present time, most studies primarily compare pre- and postintervention BP gradients as well as rates of mortality, hypertension, aneurysm formation and recoarctation to previous studies reporting the same or similar outcomes (5, 10, 13) and a relatively small fraction of studies hint that altered biomechanical properties may be present in CoA pts and contribute to the persistent morbidity discussed above (18, 23).

Further investigation into the hemodynamic and biomechanical basis of morbidity and treatment outcomes for CoA patients is particularly interesting when we consider recent advancements in computational modeling tools (9, 32, 38). Patient specific anatomy can now be extracted, and geometrically representative computational models of the vasculature can be created, using information obtained during a routine clinical imaging session (22, 27). This anatomic data can be used with phase-contrast magnetic resonance imaging (PC-MRI) and BP data to create 3D, patient-specific, time-varying representations of hemodynamics that also consider biomechanical vascular properties associated with the current patient state (8, 39). This approach has

Progress in Pediatric Cardiology, Vol. 30, No. 1-2 (December 2010): pg. 45-49. DOI.

been successfully applied to other congenital heart defects, specifically malformations resulting in a single ventricle. In these patients, computational fluid dynamics (CFD) simulations of the Fontan procedure has led to widespread acceptance of several technical modifications demonstrated to be hemodynamically superior to previous surgical techniques (25). If these techniques were applied to CoA, similar studies would likely provide greater understanding of long-term morbidity, preoperative assessment of treatment options, and an additional tool for evaluation of current treatment practices when compared to comparable results from normal patients.

What is normal anyway?

To fully characterize hemodynamic alterations associated with CoA, we must first understand related indices under normal conditions. Hemodynamic and vascular biomechanics in the thoracic aorta and its branches are complex, but particularly depend on several key factors that should be implemented when performing CFD modeling for CoA patients. Importantly, consideration of these factors allows for the replication of normal physiology and thoracic aortic anatomy and likely the greatest chance for clinical impact from an associated CFD study.

1. Blood flow patterns in the normal ascending and descending aorta range from axial during the early portion of systole, to helical during mid-to-late systole, and complex flow recirculation during end systole and diastole (15). The development of helical flow patterns during peak to late systole is thought to occur in response to the curvature of the ascending aorta and translational motion of the aortic root caused by the beating heart. Equivalent studies are currently lacking for CoA patients, likely as a result of the heterogeneity and additional cardiac abnormalities often present in this patient population. Nevertheless, simulation results should replicate flow patterns revealed by the available clinical data in order to draw reasonable conclusions.
2. The potential relationship between coarctation-related long-term morbidity and altered hemodynamics in the ascending aorta and its branches dictates that outflow boundary conditions must be selected in these vessels to replicate physiologic blood flow and BP distributions measured clinically. The reader is referred to several recent thorough articles discussing the application of realistic boundary conditions in computational models (30, 31). In addition to replicating current patient state, these physiologic outlet boundary conditions also facilitate the investigation of predictive surgical or interventional treatment planning in cases

Progress in Pediatric Cardiology, Vol. 30, No. 1-2 (December 2010): pg. 45-49. DOI.

where outflow information is not clinically available such as determining the acute response to theoretical stent implantation for the relief of CoA, or changes occurring in response to exercise.

3. The hallmark of the ascending aorta is its unique ability to store blood during systole and deliver it to the rest of the body during diastole. This property is disrupted by CoA. Therefore, computational models for use in studying CoA should consider the compliance of the aorta. This is complicated by differences in tissue properties along the length (17) and within a given circumferential region (6) of the aorta, as well as differences between the aorta and its branches (37). Although differences in these tissue properties have been previously reported for normal vasculature using experimental techniques, their estimation from non-invasive imaging and computational implementation is not trivial. The precise location and vascular influence of a particular treatment for CoA such as patch aortoplasty or balloon angioplasty is also difficult to decipher from medical imaging data. However, this information is necessary for the physiologic assessment of disease severity.
4. The aorta and innominate, carotid and subclavian arteries contain smaller branches with calibers near the detection limits of MR imaging that may be of interest for computational modeling of CoA patients. For example, the intercostal arteries are thought to take between 7 and 11% of the flow from the level of the coarctation to the level of the diaphragm under normal conditions, and are often recruited to serve as collateral vessels in patients with native CoA (26, 28). Including these vessels in a computational model (or accounting for their impact) can likely provide more physiologic results for indexes such as wall shear stress (WSS, defined as the tangential force per unit area exerted on a blood vessel wall as a result of flowing blood) throughout the descending thoracic aorta. Similarly, luminal wall motion in the ascending and descending aorta and their branches is curtailed by the presence of supporting structures including the spine, connective tissue and the intrinsic tension of arterial system that provides radial and axial tethering.
5. To be clinically applicable, the use of CFD for this application must ultimately provide unique information that is not available by other techniques. The ability of CFD to meet this criterion is somewhat inherent as it provides information that would be difficult or impossible to assess using experimental techniques. However, simply using CFD to assess blood flow and BP distributions is inadequate as current imaging and

Progress in Pediatric Cardiology, Vol. 30, No. 1-2 (December 2010): pg. 45-49. DOI.

catheterization techniques are routinely used for the same purpose. Instead investigators rely on CFD to provide estimates for indices of WSS, vascular deformation and strain and changes in these indices in response to virtual treatments or under simulated exercise conditions.

Many of the factors discussed above can be implemented using current CFD techniques while others await future progress, or are not yet ubiquitously applied, with current imaging and computational methods. Following the above review of CFD model considerations that should be implemented to replicate normal thoracic flow features and elucidate alterations in CoA patients, we now offer several examples of results from CoA patients that underwent surgical or interventional treatment.

Do previous and current treatments restore normalcy?

Traditionally surgery by resection with end-to-end anastomosis has been the gold standard for repair of CoA. While CFD has been used extensively to study possible morbidity due to altered flow conditions in smaller blood vessels prone to atherosclerosis, the potentially deleterious effects of alterations in blood flow patterns in the human thoracic aorta have not been as widely studied.

Figure 1 shows results from an ongoing investigation in which patient-specific CFD modeling was performed for control subjects and corresponding age and gender matched CoA patients that underwent surgical repair by resection with end-to-end anastomosis. Realistic inflow and outflow boundary conditions derived from PC-MRI and BP measurements were implemented to determine indices of WSS in the thoracic aorta and arteries of the head and neck. Spatiotemporal alterations in velocity streamlines, time-averaged WSS (TAWSS) and oscillatory shear index (OSI, an index of directional changes in WSS, low OSI indicates the WSS is oriented predominantly in the direction of blood flow, while a value of 0.5 is indicative of bidirectional WSS with a time-average value of zero throughout the cardiac cycle (40)) were observed for CoA patients compared to the control subjects. Axial and circumferential patterns of TAWSS and OSI for CoA patients revealed significantly higher TAWSS between 1 to 3 descending aortic diameters distal to the left subclavian artery and significantly higher OSI between 3 to 5 diameters distal to the left subclavian artery.

Progress in Pediatric Cardiology, Vol. 30, No. 1-2 (December 2010): pg. 45-49. DOI.

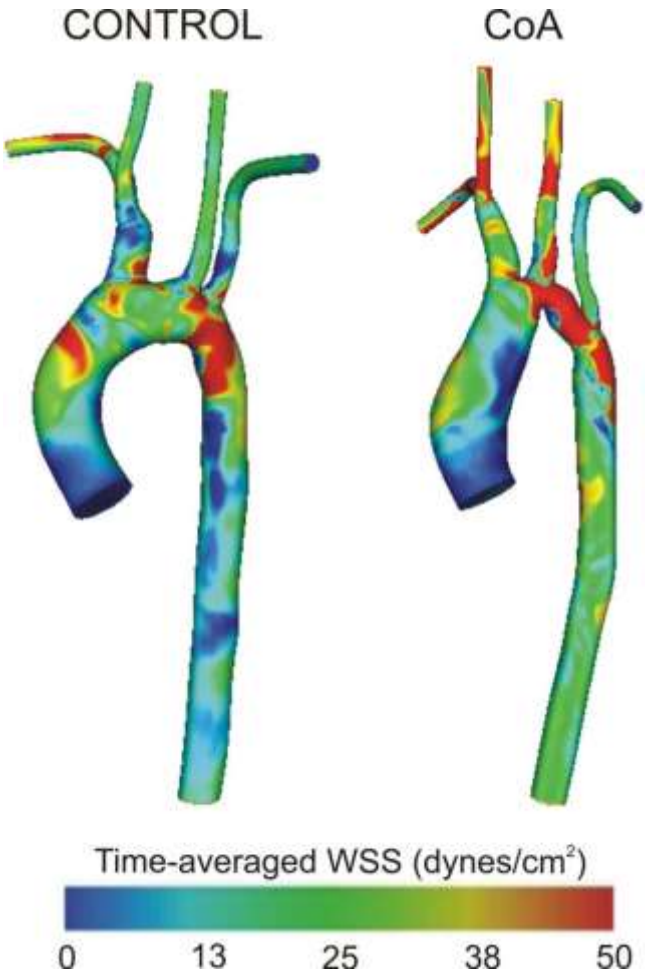

Figure 1
Spatial patterns of time-averaged WSS for an 11 yo female patient with CoA treated surgically by resection with end-to-end anastomosis repair (right) and an age and gender matched control subject (left).

In a related study (Figure 2), indices of WSS were also determined for a group of CoA patients previously surgically treated by patch aortoplasty and corresponding age- and gender-matched control patients. Heterogeneity within this CoA group is particularly striking and the presence of aneurysms in the region of ductal tissue, which is common with this repair type, can be seen in patient shown in the figure. This type of surgical correction is no longer implemented, but CFD can still be useful for planning future interventions or determining the impact of local hemodynamics on the growth and potential rupture of aneurismal corrections.

Progress in Pediatric Cardiology, Vol. 30, No. 1-2 (December 2010): pg. 45-49. DOI.

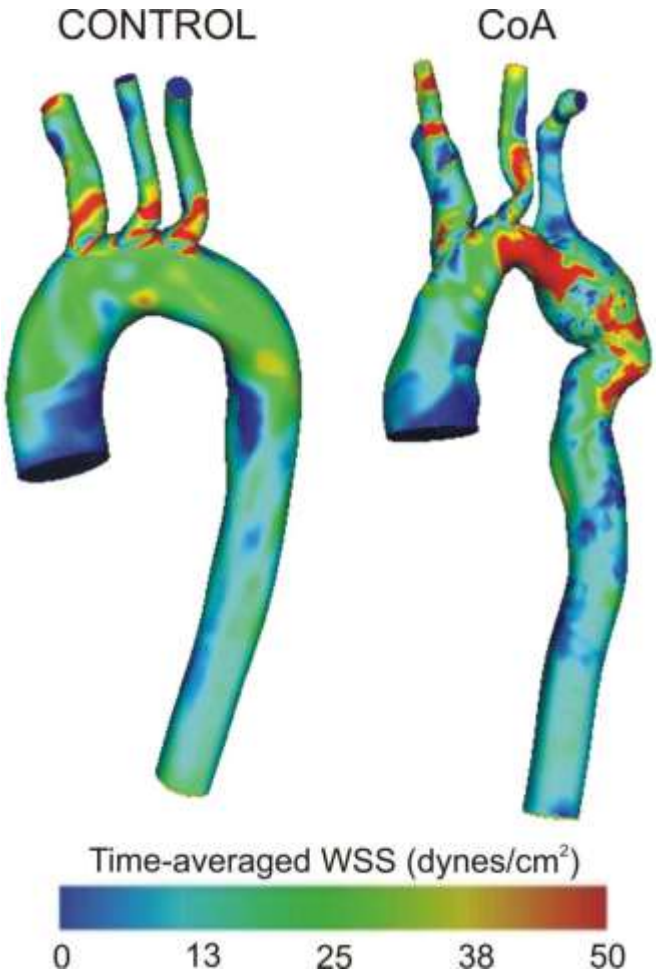

Figure 2
Spatial patterns of time-averaged WSS for a 26 yo male patient with CoA treated surgically by Dacron patch aortoplasty (right) and an age and gender matched control subject (left).

These results indicate that, in addition to any pre-existing alterations in vascular function, locations involving the surgical correction are often now those associated with potentially deleterious alterations in indices of WSS. For the studies mentioned above, the group of CoA patients undergoing surgical correction by resection and end-to-end anastomosis were younger, and therefore closer to the date of their surgical correction, than the patients from which the Dacron patch CFD models were created. While it is possible that the end-to-end repairs used for CFD modeling may undergo deleterious geometric remodeling as has occurred for many of the Dacron patch patients, the current results strongly suggest the end-to-end repair results in more favorable results from a hemodynamic perspective. Collectively these results facilitate greater understanding of the effects

of surgical repair on local hemodynamics in CoA patients by providing quantifiable values throughout the entire aorta. This data may be useful for clinicians when implementing future surgeries.

Local hemodynamics alterations after stenting for CoA

The invasive nature of surgical treatments combined with the shorter hospitalization, reduced pain and decreased cost of catheter-based therapies has led to stent implantation playing an increasing role in the treatment of CoA. Although currently there are no FDA-approved stents specifically designed for children, several stents are commonly used off-label with CoA patients and recent studies have documented some fundamental concerns regarding the use of these stents in a manner other than that for which they were intended. Among these concerns is the impact of different stent types on blood flow patterns in the descending thoracic aorta. The following example illustrates how CFD can be used to provide additional insight related to this question.

A patient-specific model was created from CT and MRI data sets obtained within several days of each other. A computational representation of the implanted stent was then created and included within the patient-specific CFD model using computer aided design software. A computational version of a second stent also commonly used in the treatment of CoA was also created and virtually implanted for comparison of downstream flow disturbances (Figure 3). The results illustrated in Figure 3 suggest there is a region of elevated TAWSS along the posterior wall of the descending thoracic aorta distal to the stents as well a difference in the amount of the anterior wall within this region that is exposed to low TAWSS. Importantly, low TAWSS is associated with the onset and progression of cardiovascular disease in many vascular beds and TAWSS above a certain preferential value may also be associated endothelial injury, plaque rupture, or thrombogenesis (12, 14). The Numed CP stent appears to be associated with a greater percentage of low TAWSS along the anterior wall and accentuate values within the region of elevated WSS along the posterior aorta, but this hypothesis remains to be tested in further detail. Additional questions pertaining to potential for the stent to cause adverse changes in the stiffness and structural components of the aorta (9), or impart residual stress on the left ventricle of the heart (16) could similarly be examined through the use of CFD.

Progress in Pediatric Cardiology, Vol. 30, No. 1-2 (December 2010): pg. 45-49. DOI.

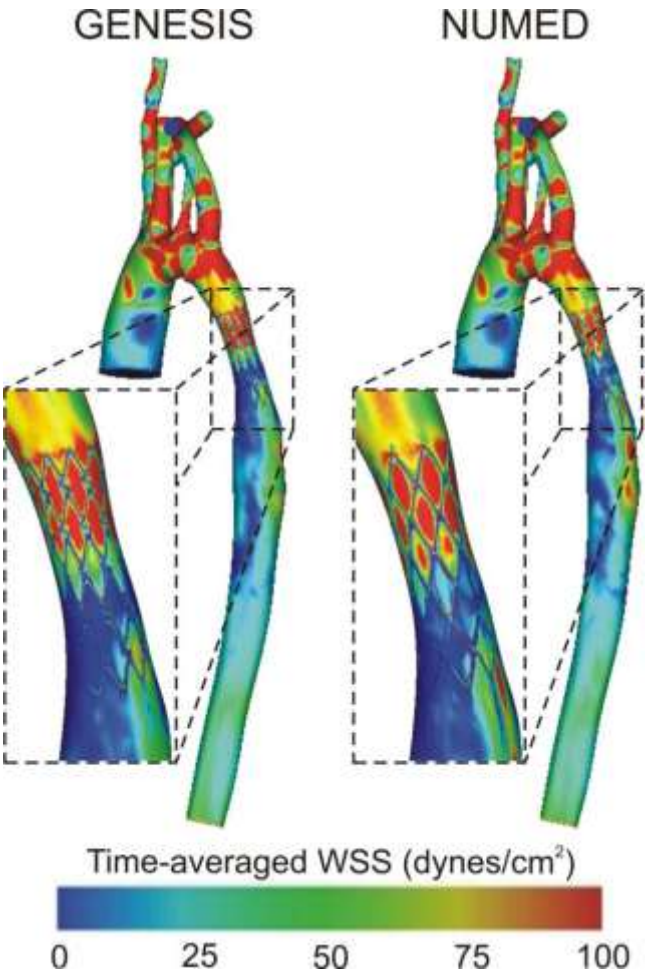

Figure 3
Time-averaged WSS results obtained from CFD models containing computational representations of two stents commonly used to treat CoA. The results reveal differences in low time-averaged WSS along the anterior wall and regions of elevated time-averaged WSS along the posterior wall of the descending thoracic aorta distal to the stents.

How does the aortic valve impact normal?

The prevalence of a bicuspid aortic valve (BAV) is ~2% in the general population (33), but 50-80% of patients diagnosed with CoA also have a BAV (33, 34). This is particularly concerning as reports have documented a nine-fold increased risk of ascending aortic dissection with BAV (33). Imaging studies using Doppler ultrasound (2) and 4D MRI flow measurements (35) have indicated BAV cause flow disturbances in the ascending aorta and progressive ascending aortic dilatation. Past studies have shown that some turbulence exists in the aortic arch (4, 15), but that diseases of the aortic valve are

almost always associated with more pronounced turbulence in the ascending aorta (29). Collectively these findings indicate the presence of a BAV in CoA patients inevitably alters hemodynamics in the ascending aorta that could lead to the progression of disease in this region and contribute to observed long-term morbidity.

As an extension of the studies discussed above, Wendell et al. (36) recently implemented idealized bicuspid and tricuspid valve morphologies into CFD models of three arch types commonly developing after surgical treatment for CoA by resection with end-to-end anastomosis (20). TAWSS, OSI, and turbulent kinetic energy (TKE) values were compared with those from an assumed parabolic inlet velocity profile. The influence of the aortic valve generally persisted into the mid-transverse arch for WSS and TKE and throughout the thoracic aorta for OSI, but varied due to features of each arch type including arch orientation, curvature and length of the ascending aortic segment. Deleterious indices of WSS (low time-averaged WSS and elevated OSI) quantified in 3 mm circumferential bands were generally more pronounced for the BAV inlet condition regardless of arch type. One of the key findings from the study was that post-surgical arch shape greatly impacts which portions of the luminal surface will be exposed to potentially subnormal values of WSS indices. Since contours for circumferential indices of WSS were generally similar across inflow types, regions of varying susceptibility resulting from surgical correction are established regardless of the number of functioning valve leaflets, but can be mitigated or worsened by valve morphology, particularly in the ascending aorta.

In vivo rabbit model of CoA

Despite notable efforts underway for the projects summarized above, the precise cause of long-term morbidity for CoA patients is difficult to assess due to the small number of patients at any institution, and their heterogeneity. A modified rabbit coarctation model was therefore created to assess hemodynamic indices including blood flow, BP and WSS caused by CoA using a coupled imaging and CFD approach. The experimental MRI protocol mirrors the protocol that was used to obtain the human MRI data sets presented above in that rabbits with surgically-induced CoA, or CoA that has been treated to mimic surgical and stent corrections, undergo MRI. The MRI data is then used to create a CFD model revealing changes in blood flow in the same manner as is being performed with the human data. Additionally, the experimental protocol provides histological results showing how changes in blood flow, BP, vessel stiffness and WSS

Progress in Pediatric Cardiology, Vol. 30, No. 1-2 (December 2010): pg. 45-49. DOI.

(Figure 4) can be associated with local structural changes in the vessel wall.

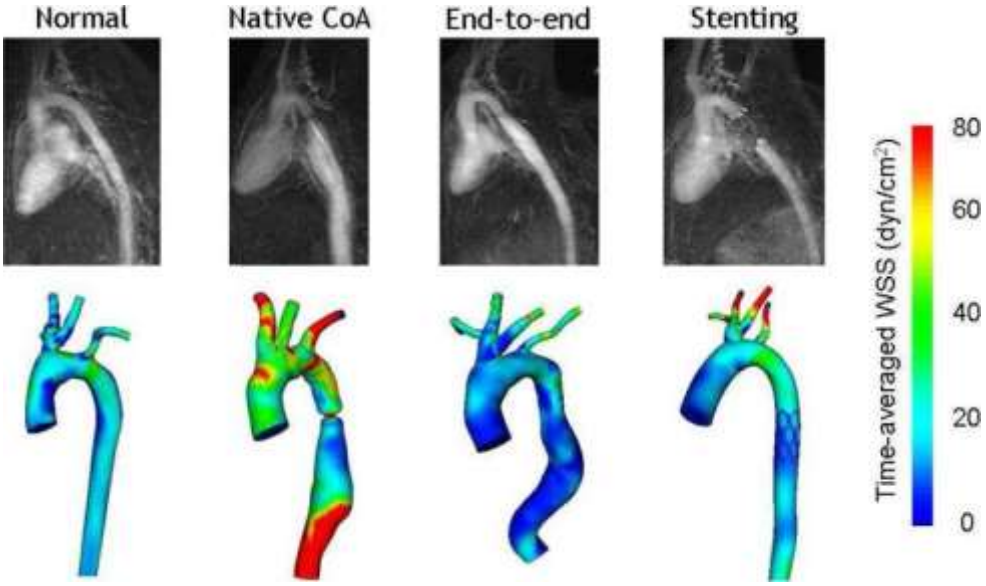

Figure 4
Representative mean intensity projections obtained from MRI angiography of the thoracic aorta of rabbits under several experimental conditions (top) with examples of corresponding CFD models (below). The experimental MRI protocol mirrors the protocol for obtaining the human MRI data used to create the CFD models shown above.

Summary

The examples discussed above show that computational simulation is currently being used to address many of the questions that persist related to treatment for CoA. Although larger studies are necessary, these recent results support the hypothesis of O'Rourke and Cartmill from nearly four decades ago. We anticipate that as the severity of hemodynamic and vascular biomechanics alterations continue to be elucidated through computational simulation, engineers and clinicians will be able to work together to identify and alleviate regions of susceptibility and, with them, potential sources of long-term morbidity for CoA patients.

Acknowledgments

The insight, collaboration, guidance and technical assistance of C. Alberto Figueroa PhD in the Department of Mechanical Engineering and Cardiovascular Biomechanics Research Laboratory at Stanford University, Irene Vignon-Clementel PhD of INRIA, and Hyun Jin Kim PhD are gratefully acknowledged. The authors would also like to especially thank Margaret Samyn MD and Joe Cave MD, PhD in the Department of Pediatrics at the Children's Hospital and Medical College of Wisconsin, and Frandics Chan MD,

PhD in the Department of Radiology at Stanford University for their clinical guidance, assistance with study design and effort obtaining medical imaging data. Ronak Dholakia MS and Sung Kwon in the Laboratory for Translational, Experimental and Computational Cardiovascular Research (CV T.E.C. Lab) at Marquette University are recognized for their assistance with CFD model construction, conducting patient-specific simulations and analysis of simulation results. Arjun Menon, Hongfeng Wang and Paul Larsen of the CV T.E.C. lab are acknowledged for their efforts and determination with the experimental rabbit model of CoA, while Dave Wendell is recognized for his work related to flow disturbances associated with the aortic valve in coarctation patients. Contributions from numerous additional clinical collaborators, academic colleagues, graduate students, post-doctoral scholars, and staff are gratefully acknowledged.

This work was partially supported by an AREA award R15HL096096-01 from the National Institutes of Health (to JFL), a pre-doctoral fellowship (0810093Z) from the American Heart Association (JFL sponsor), and assistance from the Alvin and Marion Birnschein Foundation (to JFL). Material presented here is based upon work supported by the National Science Foundation under Grant No. 0205741 (to CAT). The authors gratefully acknowledge Dr. Nathan M. Wilson for technical assistance with software development.

Footnotes

References

1. Heart Disease and Stroke Statistics - 2005 Update. American Heart Association; Dallas: p. 24.
2. Bauer M, Siniawski H, Pasic M, Schaumann B, Hetzer R. Different hemodynamic stress of the ascending aorta wall in patients with bicuspid and tricuspid aortic valve. J Card Surg. 2006;21:218–220.
3. Bobby JJ, Emami JM, Farmer RD, Newman CG. Operative survival and 40 year follow up of surgical repair of aortic coarctation. Br Heart J. 1991;65:271–276.
4. Bogren HG, Mohiaddin RH, Yang GZ, Kilner PJ, Firmin DN. Magnetic resonance velocity vector mapping of blood flow in thoracic aortic aneurysms and grafts. J Thorac Cardiovasc Surg. 1995;110:704–714.

5. Bouchart F, Dubar A, Tabley A, Litzler PY, Haas-Hubscher C, Redonnet M, Bessou JP, Soyer R. Coarctation of the aorta in adults: surgical results and long-term follow-up. Ann Thorac Surg. 2000;70:1483–1488.
6. Draney MT, Xu C, Zarins CK, Taylor CA. Circumferentially nonuniform wall thickness and lamellar structure correlates with cyclic strain in the porcine descending thoracic aorta.. ASME Summer Bioengineering Conference; Key Biscayne, FL. 2003.
7. Ferencz C, Rubin JD, McCarter RJ, Brenner JI, Neill CA, Perry LW, Hepner SI, Downing JW. Congenital heart disease: prevalence at livebirth. The Baltimore-Washington Infant Study. American Journal of Epidemiology. 1985;12:31–36.
8. Figueroa CA, LaDisa JF, Jr., Vignon-Clementel IE, Jansen KC, Hughes TJR, Feinstein JA, Taylor CA. A coupled-momentum method for fluid-structure interaction: applications to aortic coarctation.. Second International Conference on Computational Bioengineering; Lisbon, Portugal. 2005.
9. Figueroa CA, Vignon-Clementel IE, Jansen KE, Hughes TJR, Taylor CA. A coupled momentum method for modeling blood flow in three-dimensional deformable arteries. Comput Methods Appl Mech Eng. 2006;195:5685–5706.
10. Fletcher SE, Nihill MR, Grifka RG, O'Laughlin MP, Mullins CE. Balloon angioplasty of native coarctation of the aorta: midterm follow-up and prognostic factors. J Am Coll of Cardiol. 1995;25:730–734.
11. Hellenbrand WE, Allen HD, Golinko RJ, Hagler DJ, Lutin W, Kan J. Balloon angioplasty for aortic recoarctation: results of Valvuloplasty and Angioplasty of Congenital Anomalies Registry. American Journal of Cardiology. 1990;65:793–797.
12. Holme PA, Orvim U, Hamers MJ, Solum NO, Brosstad FR, Barstad RM, Sakariassen KS. Shear-induced platelet activation and platelet microparticle formation at blood flow conditions as in arteries with a severe stenosis. Arterioscler Thromb Vasc Biol. 1997;17:646–653.
13. Johnston TA, Grifka RG, Jones TK. Endovascular stents for treatment of coarctation of the aorta: acute results and follow-up experience. Catheter Cardiovasc Interv. 2004;62:499–505.
14. Karino T, Goldsmith HL. Role of blood cell-wall interactions in thrombogenesis and atherogenesis: a microrheological study. Biorheology. 1984;21:587–601.
15. Kilner PJ, Yang GZ, Mohiaddin RH, Firmin DN, Longmore DB. Helical and retrograde secondary flow patterns in the aortic arch studied by three-directional magnetic resonance velocity mapping. Circulation. 1993;88:2235–2247.
16. Kim HJ, Vignon-Clementel IE, Figueroa CA, LaDisa JF, Jansen KE, Feinstein JA, Taylor CA. On coupling a lumped parameter heart model and a three-dimensional finite element aorta model. Ann Biomed Eng. 2009;37:2153–2169.
17. Nichols WW, O'Rourke MF. McDonald's Blood Flow in Arteries: Theoretical, Experimental and Clinical Principles. Hodder Arnold; New York: 2005.
18. Ong CM, Canter CE, Gutierrez FR, Sekarski DR, Goldring DR. Increased stiffness and persistent narrowing of the aorta after successful repair of coarctation of the aorta: relationship to left ventricular mass and

blood pressure at rest and with exercise. American Heart Journal. 1992;123:1594–1600.
19. O'Rourke MF, Cartmill TB. Influence of aortic coarctation on pulsatle hemodynamics in the proximal aorta. Circulation. 1971;44:281–292.
20. Ou P, Bonnet D, Auriacombe L, Pedroni E, Balleux F, Sidi D, E. M. Late systemic hypertension and aortic arch geometry after successful repair of coarctation of the aorta. Eur Heart J. 2004;25:1853–1859.
21. Ovaert C, Benson LN, Nykanen D, Freedom RM. Transcathter treatment of coarctation of the aorta: a review. Pediatr Cardiol. 1998;19:27–44.
22. Pekkan K, Frakes D, De Zelicourt D, Lucas CW, Parks WJ, Yoganathan AP. Coupling pediatric ventricle assist devices to the Fontan circulation: simulations with a lumped-parameter model. Asaio J. 2005;51:618–628.
23. Pelech AN, Kartodihardjo W, Balfe JA, Balfe JW, Olley PM, Leenen FH. Exercise in children before and after coarctectomy: hemodynamic, echocardiographic, and biochemical assessment. Am Heart J. 1986;112:1263–1270.
24. Perloff JK. Clinical recognition of congenital heart disease. Saunders; Philadelphia: 2003. Coarctation of the aorta. pp. 113–143.
25. Pizarro C, De Leval MR. Surgical variations and flow dynamics in cavopulmonary connections: A historical review. Semin Thorac Cardiovasc Surg Pediatr Card Surg Annu. 1998;1:53–60.
26. Riehle TJ, Oshinski JN, Brummer ME, Favaloro-Sabatier J, Mahle WT, Fyfe DA, Kanter KR, Parks WJ. Velocity-encoded magnetic resonance image assessment of regional aortic flow in coarctation patients. Ann Thorac Surg. 2006;81:1002–1007.
27. Socci L, Gervaso F, Migliavacca F, Pennati G, Dubini G, Ait-Ali L, Festa P, Amoretti F, Scebba L, Luisi VS. Computational fluid dynamics in a model of the total cavopulmonary connection reconstructed using magnetic resonance images. Cardiol Young. 2005;15(Suppl 3):61–67.
28. Steffens JC, Bourne MW, Sakuma H, O'Sullivan M, Higgins CB. Quantification of collateral blood flow in coarctation of the aorta by velocity encoded cine magnetic resonance imaging. Circulation. 1994;90:937–943.
29. Stein PD, Sabbah HN. Turbulent blood flow in the ascending aorta of humans with normal and diseased aortic valves. Circ Res. 1976;39:58–65.
30. Taylor CA, Steinman DA. Image-based modeling of blood flow and vessel wall dynamics: applications, methods and future directions: Sixth International Bio-Fluid Mechanics Symposium and Workshop, March 28-30, 2008 Pasadena, California. Ann Biomed Eng. 2010;38:1188–1203.
31. Vignon-Clementel IE, Figueroa CA, Jansen KE, Taylor CA. Outflow boundary conditions for 3D simulations of non-periodic blood flow and pressure fields in deformable arteries. Comput Methods Biomech Biomed Engin. 2010;1.
32. Vignon-Clementel IE, Figueroa CA, Jansen KE, Taylor CA. Outflow boundary conditions for three-dimensional finite element modeling of blood flow and pressure in arteries. Comput Methods Appl Mech Eng. 2006;195:3776–3796.

33. Ward C. Clinical significance of the bicuspid aortic valve. Heart. 2000;83:81–85.
34. Warnes CA. Bicuspid aortic valve and coarctation: two villains part of a diffuse problem. Heart. 2003;89:965–966.
35. Weigang E, Kari FA, Beyersdorf F, Luehr M, Etz CD, Frydrychowicz A, Harloff A, Markl M. Flow-sensitive four-dimensional magnetic resonance imaging: flow patterns in ascending aortic aneurysms. Eur J Cardiothorac Surg. 2008;34:11–16.
36. Wendell DC, Samyn MM, Cava JR, Ellwein LM, Krolikowski MM, Gandy KL, Pelech AN, Shadden SC, LaDisa JFJ. Incorporating aortic valve morphology into computational fluid dynamics simulations: specific application to patients after treatment for aortic coarctation. NMR in BioMedicine submitted. 2010
37. Westerhof N, Bosman F, De Vries CJ, Noordergraaf A. Analog studies of the human systemic arterial tree. J Biomech. 1969;2:121–143.
38. Wilson N, Wang K, Dutton R, Taylor CA. A software framework for creating patient specific geometric models from medical imaging data for simulation based medical planning of vascular surgery. Lect Notes Comput Sci. 2001;2208:449–456.
39. Yeung JJ, Kim HJ, Abbruzzese TA, Vignon IE, Draney MT, Yeung KK, Perkash I, Herfkens RJ, Taylor CA, Dalman RL. Aortoiliac hemodynamic and morphologic adaptation to chronic spinal cord injury. Journal of Vascular Surgery. 2006 in press.
40. Zarins CK, Giddens DP, Bharadvaj BK, Sottiurai VS, Mabon RF, Glagov S. Carotid bifurcation atherosclerosis. Quantitative correlation of plaque localization with flow velocity profiles and wall shear stress. Circ Res. 1983;53:502–514.

Corresponding Author: John LaDisa, PhD Assistant Professor of Biomedical Engineering Marquette University Adjunct Assistant Professor of Pediatrics Children's Hospital of Wisconsin 1515 West Wisconsin Ave, room 206 Milwaukee, WI 53233

Progress in Pediatric Cardiology, Vol. 30, No. 1-2 (December 2010): pg. 45-49. DOI.